Cellular/Molecular

Differential Regulation of Action Potential- and Metabotropic Glutamate Receptor-Induced Ca^{2+} Signals by Inositol 1,4,5-Trisphosphate in Dopaminergic Neurons

Guohong Cui, Brian E. Bernier, Mark T. Harnett, and Hitoshi Morikawa

Waggoner Center for Alcohol and Addiction Research, Section of Neurobiology and Institute for Neuroscience, University of Texas, Austin, Texas 78712

Ca^{2+} signals associated with action potentials (APs) and metabotropic glutamate receptor (mGluR) activation exert distinct influences on neuronal activity and synaptic plasticity. However, it is not clear how these two types of Ca^{2+} signals are differentially regulated by neurotransmitter inputs in a single neuron. We investigated this issue in dopaminergic neurons of the ventral midbrain using brain slices. Intracellular Ca^{2+} was assessed by measuring Ca^{2+}-sensitive K^+ currents or imaging the fluorescence of Ca^{2+} indicator dyes. Tonic activation of metabotropic neurotransmitter receptors (mGluRs, α1 adrenergic receptors, and muscarinic acetylcholine receptors), attained by superfusion of agonists or weak, sustained (~1 s) synaptic stimulation, augmented AP-induced Ca^{2+} transients. In contrast, Ca^{2+} signals elicited by strong, transient (50–200 ms) activation of mGluRs with aspartate iontophoresis were suppressed by superfusion of agonists. These opposing effects on Ca^{2+} signals were both mediated by an increase in intracellular inositol 1,4,5-trisphosphate (IP_3) levels, because they were blocked by heparin, an IP_3 receptor antagonist, and reproduced by photolytic application of IP_3. Evoking APs repetitively at low frequency (2 Hz) caused inactivation of IP_3 receptors and abolished IP_3 facilitation of single AP-induced Ca^{2+} signals, whereas facilitation of Ca^{2+} signals triggered by bursts of APs (five at 20 Hz) was attenuated by less than half. We further obtained evidence suggesting that the psychostimulant amphetamine may augment burst-induced Ca^{2+} signals via both depression of basal firing and production of IP_3. We propose that intracellular IP_3 tone provides a mechanism to selectively amplify burst-induced Ca^{2+} signals in dopaminergic neurons.

Key words: **calcium (Ca); intracellular signaling; IP_3 receptor; metabotropic glutamate receptor; burst; dopaminergic neuron**

Introduction

Dopaminergic (DA) neurons in the ventral midbrain play a critical role in reward-based reinforcement learning, and maladaptive learning caused by excessive DA signals has been implicated in the development of drug addiction (Schultz, 1998; Redish, 2004). The firing of DA neurons *in vivo* switches between tonic, single-spike activity and phasic, glutamate-driven bursts (Hyland et al., 2002). DA neuron bursts giving rise to phasic DA signals in projection areas are thought to provide the "teaching signal" for reinforcement learning.

The firing pattern of neurons is determined by their intrinsic membrane properties and the synaptic inputs they receive. Intracellular Ca^{2+} ($[Ca^{2+}]_i$) is critically involved in both of these processes by regulating membrane conductances and synaptic plasticity. Ca^{2+} influx triggered by action potentials (APs) activates small-conductance Ca^{2+}-sensitive K^+ (SK) channels in DA neurons, generating large afterhyperpolarizations (AHPs) that control tonic firing frequency (Wolfart and Roeper, 2002). However, transient activation of metabotropic glutamate receptors (mGluRs) elicits release of Ca^{2+} from intracellular stores, producing a prolonged SK-mediated hyperpolarization. This hyperpolarization underlies a pause of activity that curtails phasic bursts driven by ionotropic glutamate receptors (iGluRs) (Fiorillo and Williams, 1998; Morikawa et al., 2003). Ca^{2+} signals associated with postsynaptic APs and mGluR activation also play important roles in the induction of plasticity at a variety of synapses in the CNS (Bortolotto et al., 1999; Linden, 1999; Nevian and Sakmann, 2006). Recent studies have shown that long-term potentiation (LTP) and long-term depression (LTD) of iGluR-mediated transmission can be induced in a manner dependent on postsynaptic bursts of APs and mGluR activation, respectively, in DA neurons (Bellone and Luscher, 2005; Liu et al., 2005), although other forms of plasticity have been reported using different induction protocols (Kauer, 2004; Jones and Bonci, 2005).

DA neurons receive multiple neurotransmitter inputs that activate metabotropic receptors coupled to phospholipase C (PLC)-mediated phosphoinositide (PI) hydrolysis, including mGluRs, α1 adrenergic receptors (α1ARs), and muscarinic acetylcholine receptors (mAChRs). Tonic activation of these receptors suppresses phasic mGluR-induced responses in DA neurons

Received Jan. 12, 2007; revised March 28, 2007; accepted March 28, 2007.

This work was supported by National Institutes of Health Grant DA015687. M.T.H. was supported by a National Science Foundation Graduate Research Fellowship. We thank Drs. Kamran Khodakhah, Christopher Fiorillo, and Nace Golding for comments on this manuscript and Dr. Tomokazu Doi for helpful discussions. We also thank Nicholas Gustafson for conducting some preliminary experiments.

Correspondence should be addressed to Hitoshi Morikawa, Waggoner Center for Alcohol and Addiction Research, University of Texas, 2500 Speedway, Molecular Biology Building 1.150A, Austin, TX 78712. E-mail: morikawa@mail.utexas.edu.

DOI:10.1523/JNEUROSCI.0139-07.2007

 0270-6474/07/274776-10$15.00/0

(Fiorillo and Williams, 1998, 2000; Paladini and Williams, 2004). Indeed, the psychostimulant amphetamine has been shown to inhibit mGluR-induced Ca^{2+} release via elevated extracellular DA tone activating α1ARs (Paladini et al., 2001). However, the exact intracellular mechanism mediating this inhibition remains unclear. Furthermore, it is not known how Ca^{2+} signals triggered by APs are affected by these PI-coupled neurotransmitter inputs in DA neurons.

In this study, we show that sustained activation of PI-coupled receptors augments AP-evoked Ca^{2+} transients while inhibiting phasic mGluR induced Ca^{2+} signals in DA neurons. Both of these effects are mediated by an increase in cytosolic inositol 1,4,5-trisphosphate (IP_3) levels, which facilitates Ca^{2+}-induced Ca^{2+} release (CICR) via IP_3 receptors (IP_3Rs) and, at the same time, reduces the size of Ca^{2+} stores. We further find that the facilitation of AP-induced Ca^{2+} signals is modulated by the pattern in which APs are generated, so that IP_3 selectively amplifies Ca^{2+} signals triggered by bursts of APs, but not those induced by single APs evoked at low frequency.

Materials and Methods

Slices and solutions. Horizontal slices (200–220 μm) of the ventral midbrain were prepared from adult Sprague Dawley rats (3–6 weeks old), as described previously (Cui et al., 2004). Slices were maintained at 35°C and perfused at a rate of 2–3 ml/min with physiological saline containing the following (in mM): 126 NaCl, 2.5 KCl, 1.2 NaH_2PO_4, 1.2 $MgCl_2$, 2.4 $CaCl_2$, 11 glucose, 21.4 $NaHCO_3$, saturated with 95% O_2 and 5% CO_2, pH 7.4, 300 mOsm/kg. Unless noted otherwise, pipette solutions used for whole-cell and cell-attached recordings contained the following (in mM): 115 K-methylsulfate, 20 KCl, 1.5 $MgCl_2$, 10 HEPES, 0.025 EGTA, 2 Mg-ATP, 0.2 Na_2-GTP, and 10 Na_2-phosphocreatine, pH 7.3, 280 mOsm/kg.

Electrophysiological recordings. All recordings were performed in putative DA neurons, which were identified by their large cell bodies (>20 μm) visualized with infrared-differential interference contrast optics, spontaneous firing at 1–5 Hz, and the presence of large hyperpolarization-activated I_h currents. Most (~90%) of the recordings were made in the substantia nigra pars compacta (SNc), whereas the remainder were in the ventral tegmental area (VTA). Whole-cell voltage-clamp recordings were made at a holding potential of −62 mV, corrected for a liquid junction potential of 7 mV. Series resistance (~10–20 MΩ) was continuously monitored but left uncompensated. In whole-cell current clamp recordings, small hyperpolarizing currents were injected to maintain the membrane potential at ~60 mV. MultiClamp 700A or 700B amplifiers (Molecular Devices, Union City, CA) were used to record the data, which were filtered at 1–2 kHz, digitized at 2–5 kHz, and collected using AxoGraph 4.9 (Molecular Devices) or AxoGraph X (AxoGraph Scientific, Sydney, Australia).

Iontophoretic pipettes (~100 MΩ) containing L-aspartate (1 M; pH 7.4) were placed within 5 μm of the soma or proximal dendrites. Iontophoretic pulses (50–200 nA; 50–200 ms; 0–5 nA backing current) were applied once per minute. Synaptic responses were evoked with a bipolar tungsten electrode (tip separation 100 μm) placed at 50–100 μm rostral to the recorded cell. To isolate mGluR-mediated responses, these experiments were done in slices treated with 6,7-dinitroquinoxaline-2,3-dione (DNQX; 10 μM), dizocilpine maleate (MK-801; 50 μM), picrotoxin (100 μM), (2*S*)-3-{[(1*S*)-1-(3,4-dichlorophenyl)ethyl]amino-2-hydroxypropyl}(phenylmethyl)phosphinic acid (CGP55845; 10 μM), and eticlopride (100 nM) to block AMPA, NMDA, $GABA_A$, $GABA_B$, and DA D2 receptors, respectively.

Spontaneous AP firing was monitored using either perforated-patch or cell-attached recording configurations. Perforated-patch pipettes were filled with gramicidin (50–250 μg/ml) in a solution containing 135 mM KCl and 10 mM HEPES. The firing frequency within aspartate-induced bursts was obtained by calculating the average of the second and third interspike intervals after aspartate iontophoresis.

Ca^{2+} imaging. Fluorescence imaging of $[Ca^{2+}]_i$ was made using fluo-5F (K_d = 2.3 μM) or fluo-4FF (K_d = 9.7 μM) as Ca^{2+} indicators. These indicator dyes were loaded into the cell via the whole-cell pipette. Images were taken at 15–20 Hz using a Disk Spinning Unit confocal imaging system (Olympus, Melville, NY). Ca^{2+} signals from selected regions of interest (ROIs) were expressed as follows: $\%\Delta F/F = 100 \times (F - F_{baseline})/(F_{baseline} - F_{background})$.

Flash photolysis. A 1 ms UV pulse was applied using a xenon arc lamp to elicit photolysis of caged IP_3 or caged Ca^{2+} and the resulting SK-mediated outward current was measured. The concentration of compounds photolytically released is known to be proportional to the intensity of UV pulse, which is determined by the capacitance of the capacitor in the photolysis system (Cairn Research, Faversham, UK) supplying a current to the xenon arc lamp and the voltage to which the capacitor is charged. In this study, the voltage was constantly set at 300 V and the capacitance was varied (≤4000 μF) to adjust the UV pulse intensity. The peak of the IP_3-evoked outward current (I_{IP3}) trace was not rounded even with a supramaximal intensity of UV pulse, suggesting that SK channels were not saturated by Ca^{2+}. Our previous study also demonstrated approximately linear relationship between the I_{IP3} amplitude and $[Ca^{2+}]_i$ over a wide range in DA neurons (Morikawa et al., 2000). The amplitude of I_{IP3} elicited with a supramaximal UV intensity was 350–700 pA (515 ± 37 pA; n = 10). The threshold UV intensity was defined as the largest intensity that evoked I_{IP3} <20 pA, which was routinely achieved with the capacitance in the range of 50–150 μF. This frequently resulted in no detectable I_{IP3} because of the limited resolution in setting the capacitance of the photolysis system. Caged IP_3 (100–200 μM) was loaded into the cell through the whole-cell pipette. For caged Ca^{2+}, DM-nitrophen (1.5 mM) and $CaCl_2$ (1.2 mM) were added to the whole-cell pipette.

Drugs. DNQX, MK-801, (S)-3,5-dihydroxyphenylglycine (DHPG), 2-methyl-4-carboxyphenylglycine (LY367385), CGP55845, and cyclopiazonic acid (CPA) were obtained from Tocris Bioscience (Ellisville, MO). Heparin, ruthenium red, ryanodine, and DM-nitrophen were purchased from Calbiochem (La Jolla, CA). Tetrodotoxin (TTX) was obtained from Alomone Labs (Jerusalem, Israel). Fluo-5F, fluo-4FF, and caged IP_3 were purchased from Invitrogen (San Diego, CA). All other chemicals were obtained from Sigma-RBI (St. Louis, MO).

Data analysis. Data are expressed as means ± SEM. Statistical significance was determined by Student's t test or ANOVA followed by Bonferroni's *post hoc* test. The difference was considered significant at $p < 0.05$.

Results

APs trigger CICR in DA neurons

Whole-cell voltage clamp recordings were made from DA neurons in the VTA and SNc. To assess AP-induced Ca^{2+} signals, a 2 ms depolarizing pulse of 30–60 mV was applied from a holding potential of −62 mV to evoke an unclamped AP. This produced an outward tail current lasting 150–300 ms, which was inhibited by apamin (100 nM), a blocker of Ca^{2+}-activated SK conductance (n = 33) (Fig. 1*A*). The apamin-sensitive component, termed I_{AHP}, peaked at ~20 ms after the test pulse, whereas the transient outward current insensitive to apamin mostly decayed within 20 ms. Therefore, we calculated the integral of the outward current from 20 to 300–600 ms after the test pulse to assess the charge transfer representing I_{AHP} (called Q_{AHP} hereafter). I_{AHP} was evoked in an all-or-none manner when the depolarizing pulse amplitude was varied up to 50–60 mV and was abolished by TTX (1 μM; n = 11) (supplemental Fig. S1, available at www.jneurosci.org as supplemental material). Further increasing the test pulse amplitude (n = 4) or prolonging the test pulse duration (n = 4) added a TTX-insensitive component to I_{AHP}. Thus, we routinely used a 2 ms depolarizing pulse of 30–60 mV to evoke SK-dependent I_{AHP} resulting from Ca^{2+} influx triggered by unclamped APs.

AP-induced Ca^{2+} transients can be amplified by CICR from intracellular stores via IP_3Rs and/or ryanodine receptors (RyRs) (Berridge, 1998). Consistent with this, bath application of CPA

($10–20\ \mu M$), which depletes endoplasmic reticulum Ca^{2+} stores (Smith et al., 1988), depressed Q_{AHP} by $44 \pm 3\%$ ($n = 10$) (Fig. 1*B–D*). The CPA-sensitive component of I_{AHP} peaked at 50–100 ms after the test pulse. In spontaneously firing DA neurons recorded in current clamp, CPA also reduced the AHP amplitude ($n = 3$; perforated-patch recordings) and produced a small increase in the firing frequency ($n = 9$; cell-attached or perforated-patch recordings) (supplemental Fig. S2, available at www.jneurosci.org as supplemental material). The effect of CPA on Q_{AHP} was diminished by intracellular application of heparin (1 mg/ml; $n = 5$), an IP_3R antagonist (Ghosh et al., 1988), or ruthenium red ($200\ \mu M$; $n = 8$), a RyR antagonist (Zucchi and Ronca-Testoni, 1997), and was eliminated when these two drugs were applied together ($n = 6$) (Fig. 1*B–D*). In these experiments, inclusion of heparin and/or ruthenium red in the intracellular solution tended to reduce Q_{AHP}, although this reduction was not statistically significant because of the variability in Q_{AHP} among different cells. Ryanodine ($20\ \mu M$), which locks RyR channels in a subconductance open state and thus depletes Ca^{2+} stores expressing RyRs (Zucchi and Ronca-Testoni, 1997), also produced $45 \pm 9\%$ inhibition of Q_{AHP} ($n = 6$), an effect that was blocked by ruthenium red ($-1 \pm 11\%$ inhibition; $n = 5$; $p < 0.01$ vs control). These results demonstrate that both IP_3Rs and RyRs are involved in CICR triggered by AP-induced Ca^{2+} influx.

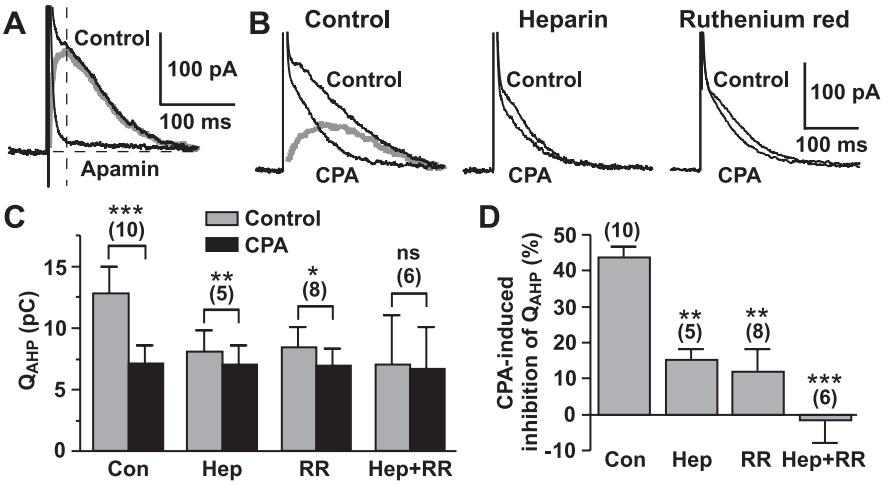

Figure 1. APs trigger Ca^{2+} release via both IP_3Rs and RyRs. ***A***, Representative traces of outward tail currents caused by an unclamped AP, evoked by a 2 ms depolarizing pulse in control and in apamin (100 nM). Apamin selectively eliminated the slow component of the tail current. The gray trace represents the I_{AHP} obtained by current subtraction. The vertical dashed line is drawn at 20 ms after the test pulse. ***B***, Representative traces illustrating the effect of CPA ($20\ \mu M$) on I_{AHP} recorded with a control (Con) internal solution, heparin (Hep; 1 mg/ml), or ruthenium red (RR; $200\ \mu M$). The gray trace in the left panel depicts the CPA-sensitive component of I_{AHP}. ***C***, Summary bar graph plotting Q_{AHP} in control and in CPA. Recordings were made with a control internal solution, heparin, ruthenium red, or both of these drugs together. $^*p < 0.05$; $^{**}p < 0.01$; $^{***}p < 0.001$; paired *t* test. ***D***, Summary bar graph plotting the effect of CPA in cells recorded with a control internal solution, heparin, ruthenium red, or both of these drugs together. $^{**}p < 0.01$; $^{***}p < 0.001$ versus control; ANOVA.

Differential regulation of AP- and phasic mGluR-induced Ca^{2+} signals by tonic activation of PI-coupled receptors

Tonic activation of PI-coupled neurotransmitter receptors, such as mGluRs, α1ARs, and mAChRs, inhibits $[Ca^{2+}]_i$ release produced by strong, phasic activation of these receptors in DA neurons (Fiorillo and Williams, 2000; Paladini et al., 2001; Morikawa et al., 2003). We thus tested whether sustained activation of these receptors could also affect the Ca^{2+} store-dependent component of I_{AHP}. In agreement with the previous studies cited above, bath perfusion of an mGluR agonist DHPG ($1\ \mu M$; $n = 4$), an α1AR agonist phenylephrine ($10\ \mu M$; $n = 7$), and an mAChR agonist muscarine ($1\ \mu M$; $n = 7$), all produced reversible inhibition of the mGluR-mediated outward current (I_{mGluR}) evoked by aspartate iontophoresis in the presence of iGluR antagonists (Fig. 2*A*,*B*,*E*). In contrast, DHPG augmented I_{AHP} by adding a slow component, which lasted up to 600 ms (Fig. 2*A*). This effect of DHPG was blocked by apamin (100 nM; $n = 3$) (Fig. 2*C*), consistent with the augmentation of AP-induced Ca^{2+} transients. On average, DHPG produced $108 \pm 17\%$ increase in Q_{AHP} ($n = 21$) (Fig. 2*E*). Furthermore, superfusion of phenylephrine and muscarine increased Q_{AHP} by $65 \pm 10\%$ ($n = 11$) and $116 \pm 25\%$ ($n = 4$), respectively (Fig. 2*D*,*E*). DHPG ($n = 2$) and phenylephrine ($n = 2$) also increased the AHP amplitude, measured in whole-cell current clamp, by ~30% (Fig. 2*D*).

We next monitored $[Ca^{2+}]_i$ by the fluorescence of fluo-5F ($50\ \mu M$). In these experiments, we evoked a train of five unclamped APs at 20 Hz to mimic burst firing of DA neurons. The burst of APs produced a rise in $[Ca^{2+}]_i$ and a summating outward current with a prolonged tail (Fig. 2*F*). The total charge transfer of this outward current, termed $Q_{AHP\text{-}burst}$, was calculated after removing a 20 ms window after each test pulse to isolate the apamin-sensitive component (Fig. 1*A*). The burst-induced Ca^{2+} signal appeared simultaneously throughout the cell but was invariably larger in proximal dendrites (~20–50 μm from the soma) than in the soma. TTX ($1\ \mu M$) abolished the burst-induced fluorescence change in dendrites and also reduced that in the soma by ~80% ($n = 7$) (supplemental Fig. S3, available at www.jneurosci.org as supplemental material). Aspartate iontophoresis produced an mGluR-mediated wave of Ca^{2+} starting at the site of application, as reported previously (Morikawa et al., 2003). Bath application of DHPG ($1\ \mu M$) increased the burst-induced fluorescence change by $75 \pm 15\%$ and decreased the mGluR-induced fluorescence change by $66 \pm 12\%$ when measured at proximal dendrites ($n = 5$) (Fig. 2*G*).

We further induced sustained activation of mGluRs by weak synaptic stimulation of glutamatergic fibers (60 stimuli at 50 Hz, starting 1 s before the onset of the burst), which evoked no detectable Ca^{2+} transient or outward current by itself (Fig. 3). Synaptic stimulation increased the burst-induced fluorescence change at the proximal dendrite close to the stimulating electrode by $59 \pm 6\%$ ($n = 2$) and $Q_{AHP\text{-}burst}$ by $60 \pm 11\%$ ($n = 3$). The facilitatory effect of synaptic stimulation was blocked by bath application of LY367385 ($50\ \mu M$), an mGluR1 antagonist ($n = 3$).

Altogether, these results show that tonic activation of PI-coupled receptors augments AP-induced Ca^{2+} transients and suppresses phasic mGluR-mediated Ca^{2+} release.

IP_3 mediates differential regulation of AP- and phasic mGluR-induced Ca^{2+} signals

To examine whether the facilitation of AP-induced Ca^{2+} signals is attained via CICR, we first used CPA to deplete Ca^{2+} stores. The effects of DHPG ($1\ \mu M$; $n = 10$) and phenylephrine ($10\ \mu M$; $n = 4$) on I_{AHP} were abolished by CPA ($10–20\ \mu M$) (Fig. 4*A*). Furthermore, the outward current produced by flash photolysis

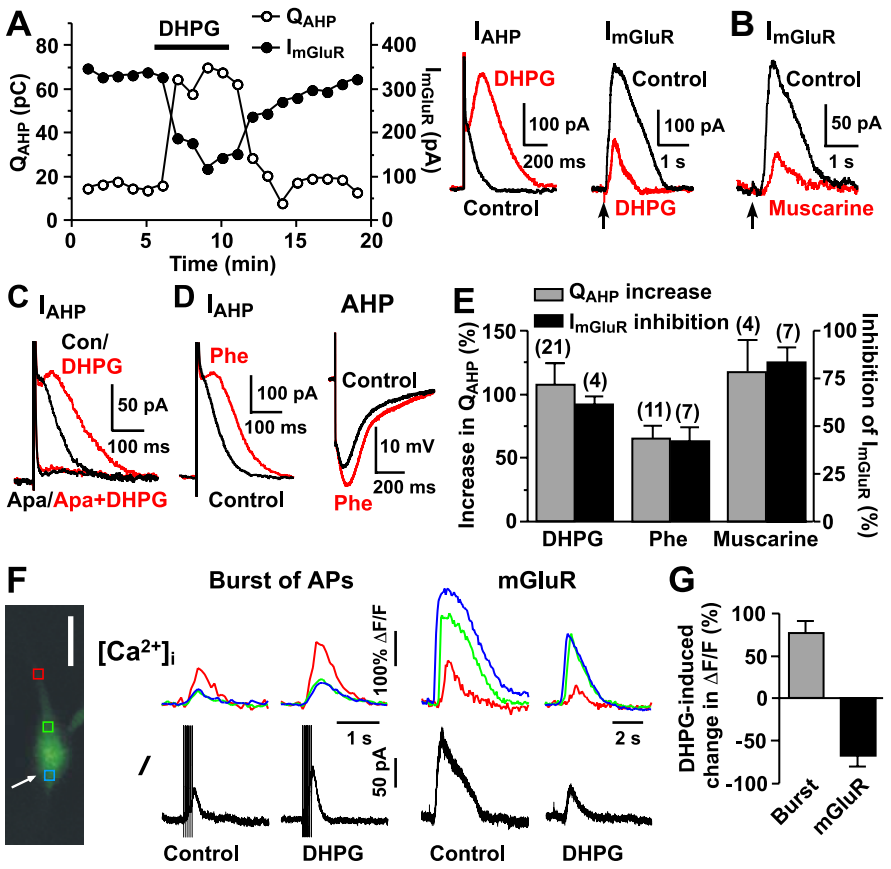

Figure 2. Sustained activation of PI-coupled receptors differentially regulates AP- and phasic mGluR-induced Ca^{2+} signals. ***A***, Time course of the opposing effects of DHPG (1 μM) on Q_{AHP} and I_{mGluR} recorded in the same cell. Representative traces of I_{AHP} and I_{mGluR} in control and in DHPG from the same experiment are shown on the right. I_{mGluR} was evoked by iontophoretic application of aspartate (100 ms) at the time indicated by the arrow. ***B***, Representative traces of I_{mGluR} in control and in muscarine (1 μM). ***C***, The effect of DHPG on I_{AHP} was blocked by apamin (Apa; 100 nM). Con, Control. ***D***, Left, Representative traces of I_{AHP} in control and in phenylephrine (Phe; 10 μM). Right, Phenylephrine also augmented AHPs recorded in the whole-cell current clamp. APs were evoked by a 2 ms current injection. ***E***, Summary bar graph showing that DHPG, phenylephrine, and muscarine all increased I_{AHP} and inhibited I_{mGluR}. ***F***, DHPG enhanced the Ca^{2+} signal induced by a burst of APs while suppressing the phasic mGluR-mediated Ca^{2+} wave. Left, A confocal fluorescence image of a DA neuron loaded with fluo-5F (50 μM) is shown. Scale bar, 20 μm. Fluorescence changes were measured at the ROIs indicated by the boxes with different color codes (top traces), while currents were recorded in the same cell (bottom traces). Middle, A train of five test pulses at 20 Hz was used to evoke a burst of five unclamped APs. Right, Aspartate was iontophoresed at the soma, as indicated by the arrow in the image at left. ***G***, Summary bar graph from five cells depicting the effects of DHPG on burst- and mGluR-induced Ca^{2+} signals measured in dendrites ~20–50 μm away from the soma.

of caged Ca^{2+} ($I_{caged\text{-}Ca}$), which directly liberates Ca^{2+} inside of the cell, was also increased by DHPG and phenylephrine in a CPA-sensitive manner (Fig. 4*B*,*C*). Although CPA itself appeared to irreversibly suppress $I_{caged\text{-}Ca}$, we did not quantify this effect because $I_{caged\text{-}Ca}$ showed rundown over time. Thus, tonic activation of PI-coupled receptors augments AP-induced Ca^{2+} signals by facilitating CICR.

G-protein-coupled metabotropic receptors can mediate the production of two Ca^{2+}-mobilizing messengers, IP_3 and cyclic ADP-ribose (cADPR), which act on IP_3Rs and RyRs, respectively (Cancela, 2001). To test the involvement of these messengers, we used heparin (1 mg/ml) to block the IP_3–IP_3R pathway and ruthenium red (200 μM) to block the cADPR–RyR pathway. DHPG-induced enhancement of I_{AHP} and suppression of I_{mGluR} were both suppressed by heparin but not by ruthenium red (Fig. 5*A*). Furthermore, the effects of phenylephrine (10 μM) and muscarine (1 μM) on I_{AHP} and I_{mGluR} were also blocked by heparin ($n = 3$ for each; data not shown). Superfusion of DHPG, phenylephrine, and muscarine all produced a small, sustained inward current (0–60 pA). This inward current was not affected by heparin or ruthenium red (data not shown), consistent with its independence from $[Ca^{2+}]_i$ mobilization (Guatteo et al., 1999). These data suggest that an increase in IP_3 tone mediates both facilitation of I_{AHP} and suppression of I_{mGluR}.

To directly demonstrate the role of IP_3, we next performed flash photolysis of caged IP_3, which releases Ca^{2+} from intracellular stores and produces an SK-mediated outward current in DA neurons (Morikawa et al., 2000). IP_3 released by a single UV pulse at threshold intensity, which barely produced an outward current by itself (<20 pA), facilitated I_{AHP} in a manner similar to perfusion of receptor agonists ($n = 5$) (Fig. 5*B*). Furthermore, I_{mGluR} was inhibited by repetitive photolytic applications of IP_3 at threshold intensity for 3 s ($n = 4$) (Fig. 5*B*), which would gradually deplete $[Ca^{2+}]_i$ stores by sustained Ca^{2+} release (Solovyova and Verkhratsky, 2003). Therefore, a small increase in cytosolic IP_3 concentration reproduced the regulation of I_{AHP} and I_{mGluR} induced by sustained activation of PI-coupled receptors. A higher concentration of DHPG (30 μM) caused inhibition of I_{AHP} instead of facilitation in five of eight cells tested (Fig. 5*C*), suggesting that higher IP_3 levels produced by strong activation of mGluRs more fully deplete Ca^{2+} stores and thus can suppress CICR triggered by APs.

Activity-dependent regulation of AP-induced Ca^{2+} signals

DA neurons tonically fire APs at 1–5 Hz and also display phasic bursts comprising 2–10 spikes at 10–50 Hz *in vivo* (Hyland et al., 2002). To investigate the regulation of AP-induced Ca^{2+} signals under more physiological conditions, I_{AHP} was evoked by a train of five test pulses at 2 Hz to mimic tonic firing. Q_{AHP} was rapidly reduced during the 2 Hz AP train (Fig. 6*A1*), from 17.3 ± 2.1 pC for the first I_{AHP} ($Q_{AHP\text{-}1}$) to 11.2 ± 2.0 pC for the fifth one ($Q_{AHP\text{-}5}$) ($n = 7$; $p < 0.01$) (Fig. 6*A2*). The reduction in Q_{AHP} during the AP train was largely eliminated in the presence of CPA (9.3 ± 2.5 pC for $Q_{AHP\text{-}1}$ vs 8.2 ± 1.9 pC for $Q_{AHP\text{-}5}$; $n = 5$; $p > 0.05$). Although CPA produced an inhibition of $Q_{AHP\text{-}5}$, the magnitude of inhibition was significantly smaller compared with that of $Q_{AHP\text{-}1}$ (45 ± 4% inhibition for $Q_{AHP\text{-}1}$ vs 26 ± 5% inhibition for $Q_{AHP\text{-}5}$; $n = 5$; $p < 0.05$) (Fig. 6*A3*). These results demonstrate that evoking APs at 2 Hz causes a decrease in AP-triggered CICR.

Surprisingly, the facilitatory effect of DHPG (1 μM) on I_{AHP} was abolished with the 2 Hz AP train (118 ± 23% increase for $Q_{AHP\text{-}1}$ vs −2 ± 4% increase for $Q_{AHP\text{-}5}$; $n = 6$; $p < 0.001$) (Fig. 6*A1*,*A4*). Consistent with this, the facilitatory effect of IP_3, photolytically applied at threshold UV intensity, was also significantly depressed by the AP train ($n = 6$; $p < 0.05$) (Fig. 7*A*,*B*).

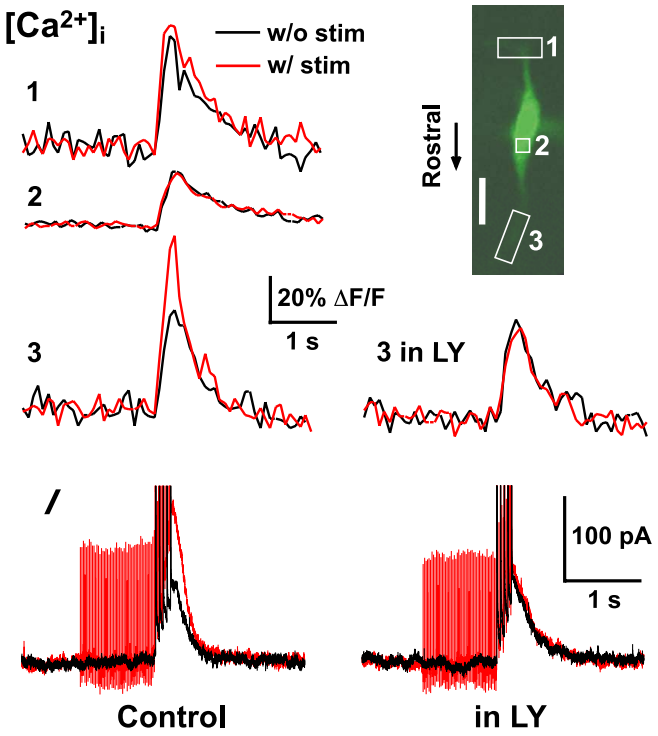

Figure 3. Synaptic activation of mGluRs facilitates burst-induced Ca^{2+} transients. A confocal fluorescence image of a DA neuron loaded with fluo-5F (50 μM) is shown on the right. Scale bar, 20 μm. A bipolar stimulating electrode was placed ~50 μm rostral to the cell for synaptic stimulation. A train of five depolarizing pulses at 20 Hz, evoking a burst of APs, was applied with (w/; red) or without (w/o; black) synaptic stimulation (stim). The synaptic stimulation consisted of 60 stimuli at 50 Hz starting 1 s before the onset of the burst. The stimulation intensity was adjusted so that synaptic stimulation alone did not induce detectable fluorescence changes. Fluorescence changes were measured at the ROIs indicated by the numbered boxes. $I_{AHP\text{-}burst}$ is shown at the bottom. Synaptic stimulation enhanced $I_{AHP\text{-}burst}$ and the burst-induced Ca^{2+} signal at the rostral dendrite close to the stimulating electrode. This enhancement was blocked by the mGluR1 antagonist, LY367385 (LY; 50 μM).

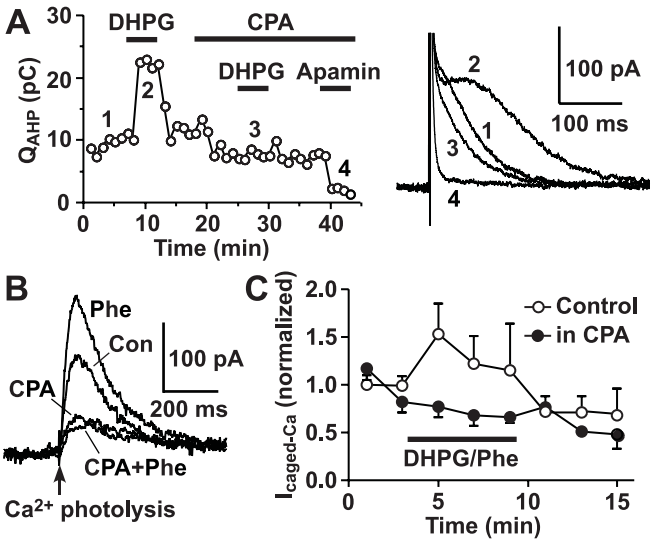

Figure 4. Tonic activation of PI-coupled receptors augments CICR. ***A***, Depleting $[Ca^{2+}]_i$ stores with CPA blocked DHPG-induced facilitation of I_{AHP}. DHPG (1 μM), CPA (10 μM), and apamin (100 nM) were perfused at the times indicated by horizontal bars. Traces of I_{AHP} at the times indicated are shown on the right. ***B***, Representative traces of $I_{caged\text{-}Ca}$ depicting the facilitating effect of phenylephrine (Phe; 10 μM) and its CPA sensitivity. Photolytic release of Ca^{2+} was made at the time indicated by the arrow. Con, Control. ***C***, Summary time graph showing that DHPG and phenylephrine augmented $I_{caged\text{-}Ca}$ in a CPA-dependent manner. $I_{caged\text{-}Ca}$ was evoked every 2 min. The amplitude of $I_{caged\text{-}Ca}$ was normalized to the average of two values before drug application. DHPG ($n = 4$ in control; $n = 2$ in CPA) and phenylephrine ($n = 3$ in control; $n = 3$ in CPA) were perfused at the time indicated by the bar. DHPG and phenylephrine data were combined and averaged.

The suppression of IP_3 facilitation of CICR may be because of inactivation or reduced sensitivity of IP_3Rs caused by $[Ca^{2+}]_i$ elevations during the AP train (Taylor and Laude, 2002). Alternatively, AP-induced CICR may reduce the size of Ca^{2+} stores to prevent further CICR. Indeed, depolarization-induced Ca^{2+} influx can either increase or reduce the Ca^{2+} store size depending on the relative rates of Ca^{2+} uptake and release (Albrecht et al., 2001). To address these possibilities, we first asked whether the AP train alters the IP_3 sensitivity of IP_3Rs. Here, we performed flash photolysis of caged IP_3 at 500 ms after the 2 Hz AP train using different intensities of UV pulse, thereby varying the concentrations of IP_3 released. The AP train had no effect on the IP_3-mediated outward current (I_{IP3}) evoked with a supramaximal UV intensity. However, the same AP train caused significant depression of I_{IP3} elicited using lower UV intensities that produced ~20% (EC_{20}) or ~50% (EC_{50}) of the maximal current amplitude (Fig. 7*C*). The magnitude of AP train-induced reduction in I_{IP3} became smaller with an increase in the UV intensity [i.e., with an increase in the IP_3 concentration (Fig. 7*E*)], indicating that high levels of IP_3 can overcome the suppression caused by the AP train. We also found that a UV intensity that was subthreshold when applied 500 ms after the AP train was able to evoke a measurable outward current when applied without the AP train, indicating that the AP train elevated the threshold for evoking I_{IP3} ($n = 3$; data not shown). In contrast, bath application of DHPG (1 μM) produced comparable inhibition of I_{IP3}

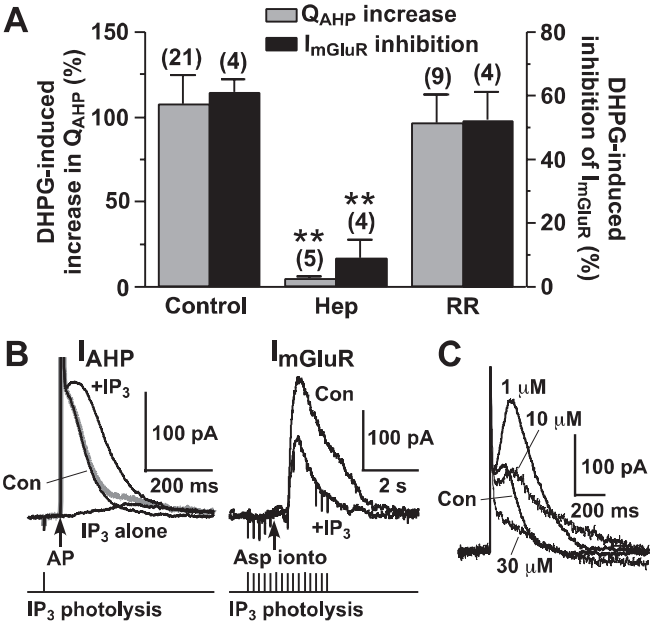

Figure 5. IP_3 mediates differential regulation of AP- and phasic mGluR-induced Ca^{2+} signals. ***A***, Summary bar graph showing the effects of DHPG (1 μM) on Q_{AHP} and I_{mGluR} in cells recorded with a control internal solution, heparin (Hep; 1 mg/ml), or ruthenium red (RR; 200 μM). $^{**}p < 0.01$ versus control; ANOVA. ***B***, Left, Representative traces of I_{AHP} with and without photolytic release of IP_3. UV flash was applied 50 ms before the 2 ms depolarizing pulse (arrow). The current elicited by IP_3 without the depolarizing pulse is also shown. The gray trace represents simple summation of control I_{AHP} and the current evoked by IP_3 alone. Right, Representative traces of I_{mGluR} with and without repetitive photolytic release of IP_3. Aspartate iontophoresis (200 ms) was made at the time indicated by the arrow. UV flash was applied at 5 Hz for 3 s, starting 1 s before aspartate iontophoresis. ***C***, Representative traces of I_{AHP} illustrating biphasic effects of DHPG at different concentrations. Con, Control.

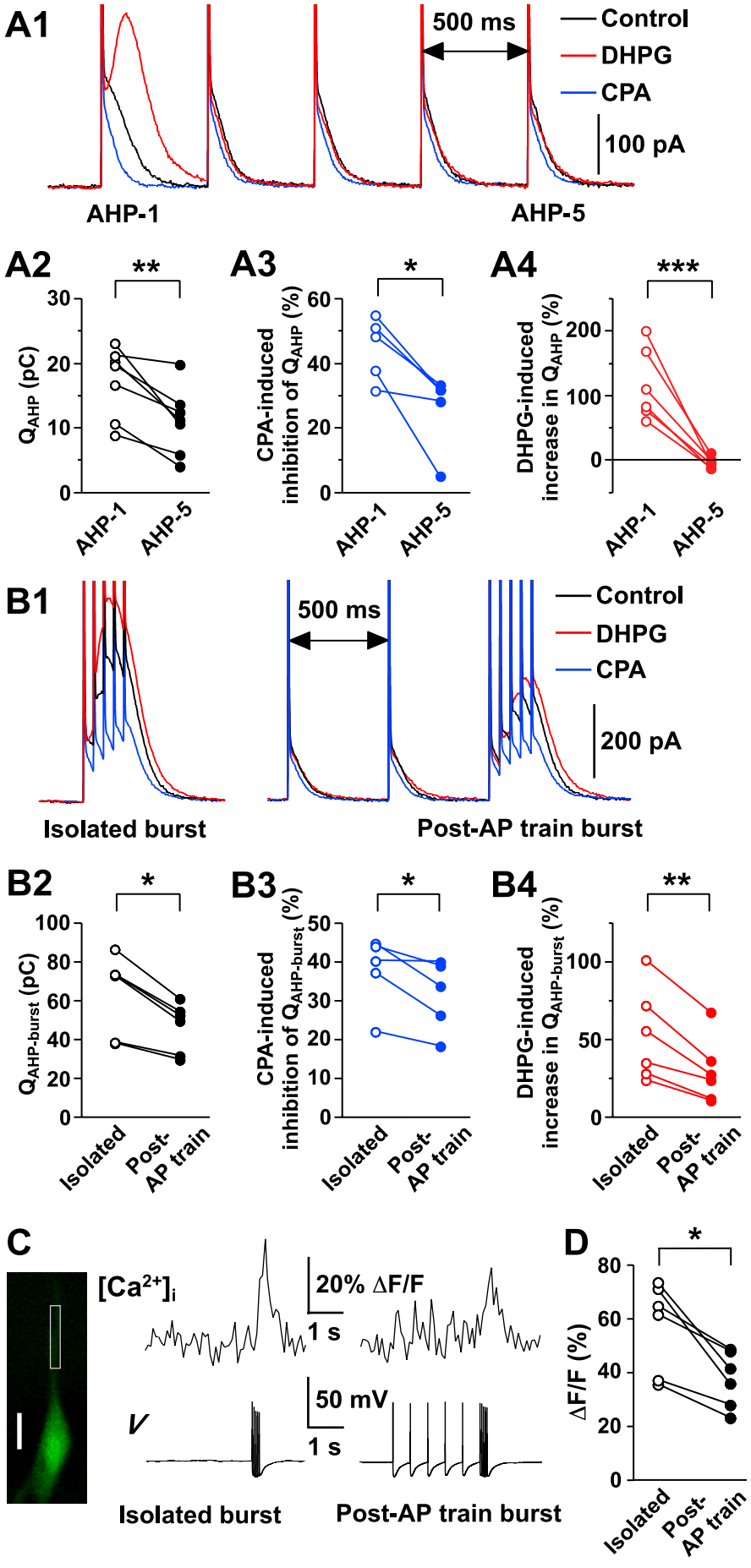

evoked by UV pulses at EC_{50} and supramaximal intensities (Fig. 7*D*,*E*). These data are consistent with the idea that (1) repetitive APs cause inactivation of IP_3Rs by reducing their IP_3 sensitivity and (2) DHPG-induced increase in IP_3 tone inhibits IP_3R-mediated Ca^{2+} release with no change in IP_3 sensitivity, as would be expected if the driving force for Ca^{2+} release is diminished by a reduction in the store Ca^{2+} concentration. Furthermore, the reduction in I_{IP3} and Q_{AHP} caused by the 2 Hz AP train recovered over a period of several seconds (Fig. 7*F*,*G*), in good agreement with the recovery kinetics of Ca^{2+}-dependent inactivation of IP_3Rs (Parker and Ivorra, 1990; Finch et al., 1991), but much faster than the time course of Ca^{2+} store replenishment that takes place over minutes (Albrecht et al., 2001; Solovyova and Verkhratsky, 2003). Altogether, these results strongly suggest that repetitive AP-induced Ca^{2+} influx produces inactivation of IP_3Rs during the AP train.

We further investigated the influence of the 2 Hz AP train on burst-induced Ca^{2+} signals. In these experiments, a burst was evoked by a train of five test pulses at 20 Hz, either in isolation or 500 ms after the 2 Hz train. As expected, $Q_{AHP\text{-}burst}$ was significantly reduced when the burst was preceded by the AP train compared with the one elicited in isolation (64.3 ± 8.4 pC for the isolated burst vs 47.0 ± 5.3 pC for the post-AP train burst; $n = 6$; $p < 0.05$)

←

Figure 6. Evoking APs at 2 Hz suppresses AP-induced CICR. ***A1***, Representative traces of I_{AHP} evoked by a train of five test pulses at 2 Hz in control (black), DHPG (1 μM; red), and CPA (10 μM; blue). ***A2–A4***, Q_{AHP}, CPA-induced inhibition of Q_{AHP}, and DHPG-induced increase in Q_{AHP} for the first (AHP-1) and fifth (AHP-5) test pulses in the AP train are plotted for each cell. Note that DHPG had no effect on $Q_{AHP\text{-}5}$. ***B1***, Representative traces of the outward current ($I_{AHP\text{-}burst}$) evoked by a train of five test pulses at 20 Hz (burst) in control (black), DHPG (red), and CPA (blue). A burst was elicited alone (isolated burst; left) or 500 ms after a 2 Hz, five-pulse train (post-AP train burst; right). The first three I_{AHP} in the AP train are not shown for clarity. Traces in A1 and B1 are from the same cell. ***B2–B4***, $Q_{AHP\text{-}burst}$, CPA-induced inhibition of $Q_{AHP\text{-}burst}$, and DHPG-induced increase in $Q_{AHP\text{-}burst}$ for the isolated burst and the post-AP train burst are plotted for each cell. Note that DHPG increased $Q_{AHP\text{-}burst}$ even for the post-AP train burst. ***C***, Evoking APs at 2 Hz suppressed the burst-induced Ca^{2+} transient. A burst was elicited alone or after a 2 Hz, five-pulse train in current clamp. APs were evoked by 2 ms current injections. A confocal fluorescence image of a DA neuron loaded with fluo-5F (50 μM) is shown on the left. Scale bar, 20 μm. Fluorescence changes were measured at the ROI indicated by the box, while the membrane potential was recorded in the same cell (bottom traces). ***D***, Fluorescence changes induced by the isolated burst and the post-AP train burst are plotted for each cell. *$p < 0.05$; **$p < 0.01$; ***$p < 0.001$; paired *t* test.

(Fig. 6*B1*,*B2*). In line with this, the AP train caused a 33 ± 5% reduction in the burst-induced fluorescence change at proximal dendrites (~20–50 μm from the soma), using fluo-5F (50 μM) or fluo-4FF (100 μM) as Ca^{2+} indicators ($n = 6$; four cells in voltage clamp and two cells in current clamp) (Fig. 6*C*,*D*). Furthermore, the effect of CPA on $Q_{AHP\text{-}burst}$ was diminished by the AP train (38 ± 4% inhibition for the isolated burst vs 32 ± 4% inhibition for the post-AP train burst; $n = 5$; $p < 0.05$) (Fig. 6*B3*), consistent with a reduction in CICR. However, DHPG, which had no effect on $Q_{AHP\text{-}5}$ in the AP train (Fig. 6*A1*,*A4*), produced a significant increase in $Q_{AHP\text{-}burst}$ after the AP train (30 ± 9% increase; $n = 6$) (Fig. 6*B1*,*B4*), although the magnitude of increase was smaller compared with that for the isolated burst (53 ± 12% increase; $p < 0.01$). These results suggest that, even if IP_3Rs are inactivated by repetitive APs, a large Ca^{2+} influx associated with a burst of APs is able to trigger IP_3R-dependent CICR when IP_3 tone is elevated.

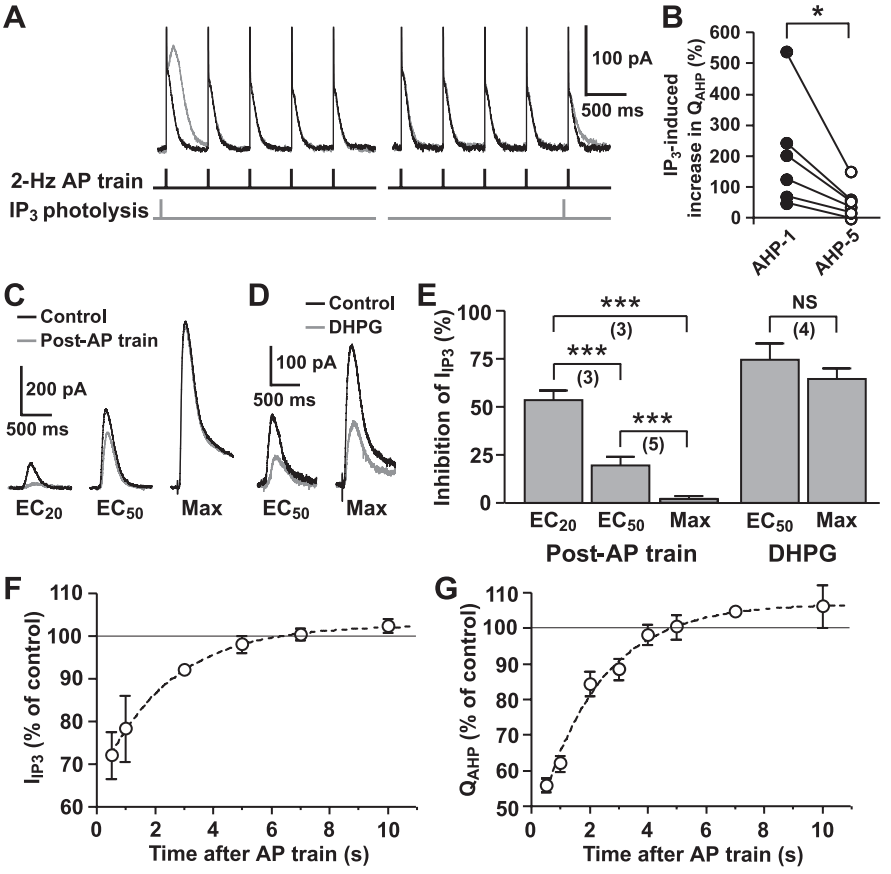

Figure 7. Repetitive APs at 2 Hz induce IP_3R inactivation. ***A***, Traces of I_{AHP} evoked by a train of five test pulses at 2 Hz with (gray) and without (black) photolytic release of IP_3. UV flash at threshold intensity was applied 50 ms before the first (left) or fifth (right) test pulse. ***B***, The magnitude of increase in Q_{AHP} by photolytic release of IP_3 at threshold intensity for the first (AHP-1) and fifth (AHP-5) test pulses in the AP train is plotted for each cell. *$p < 0.05$; paired *t* test. ***C***, Representative traces of I_{IP3} with (gray) and without (black) a preceding 2 Hz AP train. A UV flash was applied 500 ms after the fifth pulse of the train. The intensity of the UV flash was varied to elicit maximal current amplitude (Max) and ~20% (EC_{20}) or ~50% (EC_{50}) of the maximal current. ***D***, Representative traces of I_{IP3} in control (black) and in DHPG (1 μM; gray). ***E***, Summary bar graph showing the magnitude of inhibition of I_{IP3}, evoked with different UV intensities, by a 2 Hz AP train and by DHPG. Note that the AP train produced smaller inhibition as the UV intensity was increased. ***$p < 0.001$; repeated-measures ANOVA for post-AP train data and paired *t* test for DHPG data. ***F***, ***G***, The recovery time course of I_{IP3} ($n = 3$; ***F***) and Q_{AHP} ($n = 5$; ***G***) after the 2 Hz AP train. The intensity of UV flash was approximately EC_{50} for the experiments in ***F***. The dotted lines represent single exponential fit to the data.

Potential dual mechanisms of amphetamine action on burst-induced Ca^{2+} signals

The findings above imply that suppression of basal AP firing can remove IP_3R inactivation and increase the effect of IP_3. The action of psychostimulants within the DA nuclei is thought to play an important role in the development of certain behavioral adaptations underlying addiction (Kauer, 2004; Jones and Bonci, 2005). It is well known that the psychostimulant amphetamine suppresses tonic, single-spike firing via activation of D2 autoreceptors (Mercuri et al., 1989), an effect that should increase burst-induced Ca^{2+} signals and their IP_3-mediated facilitation by removing IP_3R inactivation. However, it is not clear how amphetamine affects burst firing itself. To address this issue, we performed cell-attached recordings of DA neuron firing (Fig. 8*A1*). Iontophoretic application of aspartate elicited an iGluR-mediated burst followed by an mGluR-mediated pause, as reported previously (Morikawa et al., 2003). Bath application of amphetamine (10 μM) for ~3 min decreased the basal firing frequency by 86 ± 3% (from 2.4 ± 0.2 to 0.3 ± 0.1 Hz; $n = 5$) (Fig. 8*A1*,*A2*). However, amphetamine produced only a small inhibition of the firing frequency within bursts (27 ± 4% inhibition, from 19.0 ± 3.1 to 13.8 ± 2.3 Hz) and the number of spikes per burst (26 ± 3% inhibition, from 7.4 ± 0.6 to 5.4 ± 0.3). These data demonstrate that amphetamine spares burst firing compared with its massive inhibition of tonic firing.

Amphetamine-induced dopamine release can also activate α1ARs in DA neurons (Paladini et al., 2001; Cui et al., 2004). Therefore, it is possible that amphetamine augments burst-induced Ca^{2+} signals via both D2-mediated inhibition of basal firing and α1AR-mediated facilitation of CICR. To test this possibility, we first examined how amphetamine-induced change in the firing pattern affects burst-evoked Ca^{2+} signals. In these experiments, I_{AHP} was elicited using two different protocols: (1) a control protocol simulating the firing pattern under control conditions (seven test pulses at 19 Hz for the burst, preceded by five test pulses at 2.4 Hz for the basal firing) and (2) an amphetamine protocol mimicking the firing pattern in amphetamine (five test pulses at 14 Hz for the burst, preceded by two test pulses at 0.3 Hz for the basal firing) (Fig. 8*B1*). $Q_{AHP\text{-}burst}$ induced using the amphetamine protocol was significantly larger than that elicited with the control protocol (44 ± 11% increase; $n = 11$) (Fig. 8*B2*). Phenylephrine (10 μM) superfused, whereas evoking I_{AHP} with the amphetamine protocol further increased $Q_{AHP\text{-}burst}$ by 17 ± 5% ($n = 5$). These results suggest that amphetamine can augment burst-induced Ca^{2+} signals via both suppression of basal AP firing and IP_3-mediated facilitation of CICR.

Discussion

By measuring the Ca^{2+}-sensitive SK conductance and the fluorescence of Ca^{2+} indicator dyes, we have demonstrated that tonic activation of PI-coupled receptors enhances AP-evoked Ca^{2+} transients while inhibiting Ca^{2+} signals caused by phasic mGluR

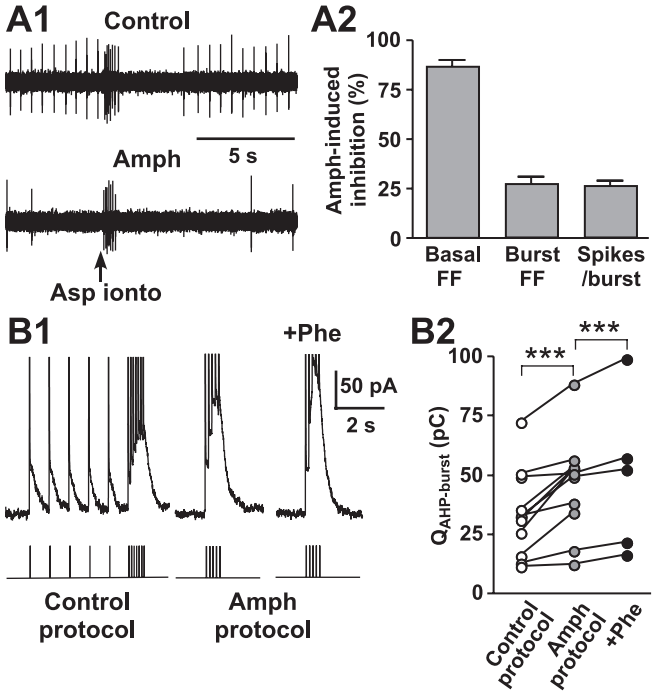

Figure 8. Amphetamine may augment burst-evoked Ca^{2+} signals via dual mechanisms. ***A1***, Representative traces of DA neuron firing in control and in amphetamine (Amph; 10 μM) recorded with a cell-attached configuration. The burst was elicited by iontophoretic (ionto) application of aspartate (50 ms). ***A2***, Summary bar graph illustrating that amphetamine suppressed basal firing frequency (FF) with relatively small effects on burst firing. The data are from five cells. ***B1***, Representative traces of $I_{AHP\text{-}burst}$ generated by a control protocol simulating the firing pattern under control conditions (19 Hz; 7 AP burst preceded by 5 APs at 2.4 Hz; left) and by an amphetamine protocol mimicking the firing pattern in amphetamine (14 Hz, 5 AP burst preceded by 2 APs at 0.33 Hz; middle). A trace of $I_{AHP\text{-}burst}$ evoked by the amphetamine protocol in the presence of phenylephrine (10 μM) is also shown on the right. All three traces are from the same cell. ***B2***, $Q_{AHP\text{-}burst}$ of individual cells recorded under three different conditions as in ***B1***. Switching from the control protocol to the amphetamine protocol induced a significant increase in $Q_{AHP\text{-}burst}$, which was further augmented by phenylephrine. ***$p < 0.001$; repeated-measures ANOVA.

activation in DA neurons. A small rise in intracellular IP_3 tone, causing (1) sensitization of IP_3Rs to Ca^{2+}-dependent activation and (2) partial depletion of $[Ca^{2+}]_i$ stores, is responsible for these effects. This differential regulation is also tuned by the context in which APs are generated, in a manner that selectively amplifies burst-induced Ca^{2+} signals in tonically firing DA neurons. These findings provide important mechanistic insights into the regulation of Ca^{2+} signals by metabotropic neurotransmitter inputs and neuronal activity.

IP_3 mediates differential regulation

Our results show that APs trigger CICR through both IP_3Rs and RyRs under resting conditions. IP_3Rs and RyRs are each coactivated by Ca^{2+} and another intracellular messenger: IP_3 for IP_3Rs and cADPR for RyRs (Berridge, 1998). Accordingly, a rise in IP_3 or cADPR levels can augment AP-induced CICR via IP_3Rs or RyRs (Hua et al., 1994; Nakamura et al., 2000). Previous studies have shown that both IP_3 and cADPR contribute to Ca^{2+} release produced by strong, transient activation of mGluRs and α1ARs in DA neurons (Morikawa et al., 2003; Paladini and Williams, 2004). However, only the IP_3 pathway was involved in the facilitation of CICR, as well as in the inhibition of transient mGluR-induced Ca^{2+} release, produced by relatively weak, sustained activation of these receptors. It is likely that the cADPR concentration did not reach levels necessary to coactivate RyRs with Ca^{2+} or to induce continuous Ca^{2+} leak via RyRs causing partial depletion of Ca^{2+} stores. It has been shown that pharmacological blockade of the PLC–IP_3 pathway suppresses the enhancement of AP-induced Ca^{2+} responses by metabotropic receptors in other central neurons (Pan et al., 1994; Nakamura et al., 1999; Power and Sah, 2002). Our data showing that direct photolytic application of IP_3 can reproduce the effect of receptor activation provide strong support for the role of IP_3 in this process.

Strong, focal activation of mGluRs elicits a slowly propagating Ca^{2+} wave in DA neurons as well as in hippocampal and cortical pyramidal neurons (Nakamura et al., 1999; Larkum et al., 2003; Morikawa et al., 2003), likely reflecting the diffusion of IP_3/cADPR or Ca^{2+}. In contrast, Ca^{2+} transients evoked by a burst of APs occurred simultaneously at the soma and proximal dendrites, which were enhanced by DHPG in terms of both the amplitude and duration. This observation suggests that IP_3 tone developed throughout the cell facilitated CICR triggered by rapidly propagating APs (Hausser et al., 1995). However, the amplitude of Ca^{2+} transients, as well as the magnitude of DHPG-induced enhancement, was larger in proximal dendrites than in the soma. Although the reason for this difference is uncertain, it is likely to result, at least partly, from the large volume of the soma diluting Ca^{2+} and/or IP_3 (Watanabe et al., 2006). Consistent with this idea, weak, sustained synaptic stimulation of mGluRs facilitated burst-induced Ca^{2+} signals only in the proximal dendrite close to the stimulating electrode but not in the soma or the opposite dendrite.

Our result showing that DHPG inhibits I_{IP3} without changing the IP_3 sensitivity suggests a reduction in the size of Ca^{2+} stores. It should also be noted that DHPG-induced inhibition of I_{mGluR} slowly recovered over a period of ~10 min after washout of DHPG, likely reflecting slow replenishment of Ca^{2+} stores (Solovyova and Verkhratsky, 2003). It has been shown that IP_3Rs and RyRs are expressed on a common pool of Ca^{2+} stores in DA neurons (Morikawa et al., 2000). Recent evidence further suggests that the endoplasmic reticulum in DA neurons may actually be a single, interconnected lumen (Choi et al., 2006). Therefore, IP_3 tone produced by sustained receptor activation likely affects the entire pool of Ca^{2+} stores. In line with this, our previous study has demonstrated that sustained activation of α1ARs suppresses RyR-mediated spontaneous Ca^{2+} responses observed in DA neurons of neonatal rats (Cui et al., 2004).

Repetitive APs inactivates IP_3Rs

IP_3Rs are biphasically regulated by cytosolic Ca^{2+} (Taylor and Laude, 2002). Compared with rapid Ca^{2+}-dependent activation of IP_3Rs, inactivation induced by Ca^{2+} has a slow rate of onset (hundreds of milliseconds) and lasts for seconds (Parker and Ivorra, 1990; Finch et al., 1991; Doi et al., 2005). A previous study has shown that repetitive firing of DA neurons produces elevations of $[Ca^{2+}]_i$ up to ~250 nM (Wilson and Callaway, 2000), which may well cause Ca^{2+}-dependent inactivation of IP_3Rs. Indeed, evoking APs at 2 Hz suppressed IP_3R-mediated CICR in this study. It should be noted that during the 2 Hz AP train, AP-triggered CICR was fully suppressed when the second AP was evoked (i.e., 500 ms after the first AP) both in the control and in DHPG. Furthermore, this reduction fully recovered in 5–10 s. These observations are in good agreement with the kinetics of IP_3R inactivation described above. We further found that IP_3R inactivation caused by repetitive APs was associated with a decrease in IP_3 sensitivity, consistent with previous studies demon-

strating reduced IP_3 binding affinity when IP_3Rs are inactivated by Ca^{2+} (Joseph et al., 1989; Moraru et al., 1999).

It has been reported that IP_3Rs inactivated by a low concentration of Ca^{2+} (250 nM) can still be activated by a higher concentration of Ca^{2+} (1 μM) in the presence of a constant level of IP_3 (Finch et al., 1991). In line with this, a large Ca^{2+} influx produced by a burst of APs was able to trigger CICR through IP_3Rs even when they were inactivated by repetitive APs. Importantly, this property enables tonic activation of PI-coupled receptors to selectively amplify burst-induced Ca^{2+} signals when DA neurons are constantly firing at low frequency.

In contrast to the suppression of AP-induced CICR and/or IP_3R-mediated Ca^{2+} release caused by repetitive APs in this study, tonic firing of DA neurons for a relatively prolonged period (20–50 s) has been shown to augment mGluR-mediated Ca^{2+} release after the firing is stopped by a hyperpolarizing current injection (Fiorillo and Williams, 1998). This augmentation, which is most likely because of loading of Ca^{2+} stores by AP-induced Ca^{2+} influx (Stutzmann et al., 2003; Watanabe et al., 2006), is largest at ~10 s after the injection of hyperpolarizing current and gradually declines over 1–2 min. The apparent discrepancy can be accounted for by the persistence of store loading, which can last for several minutes (Pozzo-Miller et al., 2000), much longer than the Ca^{2+}-dependent IP_3R inactivation that recovers in seconds. In our study, I_{IP3}/I_{AHP} reduced during the 2 Hz, five-AP train did not show much over-recovery above the control level after a 10 s interval, suggesting that the short (2 s) AP train produced little store loading.

In this study, amphetamine suppressed tonic firing with only a small inhibitory effect on iGluR-induced bursts, suggesting that the iGluR-mediated excitatory drive can largely overcome the D2-mediated inhibition. A recent report also showed that cocaine had similar differential effects on basal firing and evoked bursts *in vivo* (Almodovar-Fabregas et al., 2002). Amphetamine exerts two opposing actions on DA neuron activity: D2 autoreceptor-mediated inhibition and α1AR-mediated excitation (Mercuri et al., 1989; Shi et al., 2000; Paladini et al., 2001). Our study demonstrates that these two receptors can cooperate to selectively augment burst-induced Ca^{2+} signals. Here, D2-mediated suppression of basal firing removes Ca^{2+}-dependent inactivation of IP_3Rs, thereby boosting the facilitation of CICR via α1AR-mediated production of IP_3 tone.

Functional significance: potential relevance to synaptic plasticity

It has been shown recently that LTP and LTD of iGluR-mediated transmission can be induced in a manner dependent on postsynaptic bursts of APs and mGluR activation, respectively, in DA neurons (Bellone and Luscher, 2005; Liu et al., 2005). A rise in $[Ca^{2+}]_i$ is ubiquitously involved in the induction of LTP dependent on postsynaptic APs (Linden, 1999; Nevian and Sakmann, 2006). Furthermore, the mGluR-dependent LTD in DA neurons is blocked by the Ca^{2+} chelator BAPTA, suggesting the role of mGluR-mediated Ca^{2+} release (Bellone and Luscher, 2005). Thus, an increase in intracellular IP_3 levels may shift the balance of DA neuron plasticity toward LTP by selectively amplifying burst-induced Ca^{2+} signals while suppressing mGluR-induced Ca^{2+} release.

Weak, sustained stimulation of glutamatergic fibers effectively facilitated burst-induced Ca^{2+} transients via mGluR activation in this study. DA neurons also receive other neurotransmitter inputs activating PI-coupled receptors. These include noradrenergic, cholinergic, and peptidergic inputs, which can all act through volume transmission (i.e., through a rise in extracellular tone) and are involved in behavioral arousals (Grace et al., 1998; Fiorillo and Williams, 2000; Ungless et al., 2003; Borgland et al., 2006). Recent studies further demonstrate the role of PI-coupled receptors on DA neurons in the behavioral and pharmacological responses to psychostimulants (Paladini et al., 2001; Ungless et al., 2003; Borgland et al., 2006). By promoting the potentiation of glutamatergic transmission onto DA neurons, the differential regulation of Ca^{2+} signals described in this study may contribute to enhanced reinforcement learning when animals are placed in behaviorally arousing environments or exposed to psychostimulants.

References

Albrecht MA, Colegrove SL, Hongpaisan J, Pivovarova NB, Andrews SB, Friel DD (2001) Multiple modes of calcium-induced calcium release in sympathetic neurons I: attenuation of endoplasmic reticulum Ca^{2+} accumulation at low $[Ca^{2+}](i)$ during weak depolarization. J Gen Physiol 118:83–100.

Almodovar-Fabregas LJ, Segarra O, Colon N, Dones JG, Mercado M, Mejias-Aponte CA, Vazquez R, Abreu R, Vazquez E, Williams JT, Jimenez-Rivera CA (2002) Effects of cocaine administration on VTA cell activity in response to prefrontal cortex stimulation. Ann NY Acad Sci 965:157–171.

Bellone C, Luscher C (2005) mGluRs induce a long-term depression in the ventral tegmental area that involves a switch of the subunit composition of AMPA receptors. Eur J Neurosci 21:1280–1288.

Berridge MJ (1998) Neuronal calcium signaling. Neuron 21:13–26.

Borgland SL, Taha SA, Sarti F, Fields HL, Bonci A (2006) Orexin A in the VTA is critical for the induction of synaptic plasticity and behavioral sensitization to cocaine. Neuron 49:589–601.

Bortolotto ZA, Fitzjohn SM, Collingridge GL (1999) Roles of metabotropic glutamate receptors in LTP and LTD in the hippocampus. Curr Opin Neurobiol 9:299–304.

Cancela JM (2001) Specific Ca2+ signaling evoked by cholecystokinin and acetylcholine: the roles of NAADP, cADPR, and IP3. Annu Rev Physiol 63:99–117.

Choi YM, Kim SH, Chung S, Uhm DY, Park MK (2006) Regional interaction of endoplasmic reticulum Ca2+ signals between soma and dendrites through rapid luminal Ca^{2+} diffusion. J Neurosci 26:12127–12136.

Cui G, Okamoto T, Morikawa H (2004) Spontaneous opening of T-type Ca^{2+} channels contributes to the irregular firing of dopamine neurons in neonatal rats. J Neurosci 24:11079–11087.

Doi T, Kuroda S, Michikawa T, Kawato M (2005) Inositol 1,4,5-trisphosphate-dependent Ca^{2+} threshold dynamics detect spike timing in cerebellar Purkinje cells. J Neurosci 25:950–961.

Finch EA, Turner TJ, Goldin SM (1991) Calcium as a coagonist of inositol 1,4,5-trisphosphate-induced calcium release. Science 252:443–446.

Fiorillo CD, Williams JT (1998) Glutamate mediates an inhibitory postsynaptic potential in dopamine neurons. Nature 394:78–82.

Fiorillo CD, Williams JT (2000) Cholinergic inhibition of ventral midbrain dopamine neurons. J Neurosci 20:7855–7860.

Ghosh TK, Eis PS, Mullaney JM, Ebert CL, Gill DL (1988) Competitive, reversible, and potent antagonism of inositol 1,4,5-trisphosphate-activated calcium release by heparin. J Biol Chem 263:11075–11079.

Grace AA, Gerfen CR, Aston-Jones G (1998) Catecholamines in the central nervous system. Overview. Adv Pharmacol 42:655–670.

Guatteo E, Mercuri NB, Bernardi G, Knopfel T (1999) Group I metabotropic glutamate receptors mediate an inward current in rat substantia nigra dopamine neurons that is independent from calcium mobilization. J Neurophysiol 82:1974–1981.

Hausser M, Stuart G, Racca C, Sakmann B (1995) Axonal initiation and active dendritic propagation of action potentials in substantia nigra neurons. Neuron 15:637–647.

Hua SY, Tokimasa T, Takasawa S, Furuya Y, Nohmi M, Okamoto H, Kuba K (1994) Cyclic ADP-ribose modulates Ca2+ release channels for activation by physiological Ca2+ entry in bullfrog sympathetic neurons. Neuron 12:1073–1079.

Hyland BI, Reynolds JN, Hay J, Perk CG, Miller R (2002) Firing modes of midbrain dopamine cells in the freely moving rat. Neuroscience 114:475–492.

Jones S, Bonci A (2005) Synaptic plasticity and drug addiction. Curr Opin Pharmacol 5:20–25.

Joseph SK, Rice HL, Williamson JR (1989) The effect of external calcium and pH on inositol trisphosphate-mediated calcium release from cerebellum microsomal fractions. Biochem J 258:261–265.

Kauer JA (2004) Learning mechanisms in addiction: synaptic plasticity in the ventral tegmental area as a result of exposure to drugs of abuse. Annu Rev Physiol 66:447–475.

Larkum ME, Watanabe S, Nakamura T, Lasser-Ross N, Ross WN (2003) Synaptically activated Ca2+ waves in layer 2/3 and layer 5 rat neocortical pyramidal neurons. J Physiol (Lond) 549:471–488.

Linden DJ (1999) The return of the spike: postsynaptic action potentials and the induction of LTP and LTD. Neuron 22:661–666.

Liu QS, Pu L, Poo MM (2005) Repeated cocaine exposure in vivo facilitates LTP induction in midbrain dopamine neurons. Nature 437:1027–1031.

Mercuri NB, Calabresi P, Bernardi G (1989) The mechanism of amphetamine-induced inhibition of rat substantia nigra compacta neurones investigated with intracellular recording in vitro. Br J Pharmacol 98:127–134.

Moraru II, Kaftan EJ, Ehrlich BE, Watras J (1999) Regulation of type 1 inositol 1,4,5-trisphosphate-gated calcium channels by InsP3 and calcium: simulation of single channel kinetics based on ligand binding and electrophysiological analysis. J Gen Physiol 113:837–849.

Morikawa H, Imani F, Khodakhah K, Williams JT (2000) Inositol 1,4,5-triphosphate-evoked responses in midbrain dopamine neurons. J Neurosci 20:RC103.

Morikawa H, Khodakhah K, Williams JT (2003) Two intracellular pathways mediate metabotropic glutamate receptor-induced Ca^{2+} mobilization in dopamine neurons. J Neurosci 23:149–157.

Nakamura T, Barbara JG, Nakamura K, Ross WN (1999) Synergistic release of Ca2+ from IP3-sensitive stores evoked by synaptic activation of mGluRs paired with backpropagating action potentials. Neuron 24:727–737.

Nakamura T, Nakamura K, Lasser-Ross N, Barbara JG, Sandler VM, Ross WN (2000) Inositol 1,4,5-trisphosphate (IP3)-mediated Ca^{2+} release evoked by metabotropic agonists and backpropagating action potentials in hippocampal CA1 pyramidal neurons. J Neurosci 20:8365–8376.

Nevian T, Sakmann B (2006) Spine Ca^{2+} signaling in spike-timing-dependent plasticity. J Neurosci 26:11001–11013.

Paladini CA, Williams JT (2004) Noradrenergic inhibition of midbrain dopamine neurons. J Neurosci 24:4568–4575.

Paladini CA, Fiorillo CD, Morikawa H, Williams JT (2001) Amphetamine selectively blocks inhibitory glutamate transmission in dopamine neurons. Nat Neurosci 4:275–281.

Pan ZZ, Grudt TJ, Williams JT (1994) Alpha 1-adrenoceptors in rat dorsal raphe neurons: regulation of two potassium conductances. J Physiol (Lond) 478:437–447.

Parker I, Ivorra I (1990) Inhibition by Ca2+ of inositol trisphosphate-mediated Ca2+ liberation: a possible mechanism for oscillatory release of Ca2+. Proc Natl Acad Sci USA 87:260–264.

Power JM, Sah P (2002) Nuclear calcium signaling evoked by cholinergic stimulation in hippocampal CA1 pyramidal neurons. J Neurosci 22:3454–3462.

Pozzo-Miller LD, Connor JA, Andrews SB (2000) Microheterogeneity of calcium signalling in dendrites. J Physiol (Lond) 525:53–61.

Redish AD (2004) Addiction as a computational process gone awry. Science 306:1944–1947.

Schultz W (1998) Predictive reward signal of dopamine neurons. J Neurophysiol 80:1–27.

Shi WX, Pun CL, Zhang XX, Jones MD, Bunney BS (2000) Dual effects of D-amphetamine on dopamine neurons mediated by dopamine and non-dopamine receptors. J Neurosci 20:3504–3511.

Smith JS, Imagawa T, Ma J, Fill M, Campbell KP, Coronado R (1988) Purified ryanodine receptor from rabbit skeletal muscle is the calcium-release channel of sarcoplasmic reticulum. J Gen Physiol 92:1–26.

Solovyova N, Verkhratsky A (2003) Neuronal endoplasmic reticulum acts as a single functional Ca2+ store shared by ryanodine and inositol-1,4,5-trisphosphate receptors as revealed by intra-ER [Ca2+] recordings in single rat sensory neurones. Pflügers Arch 446:447–454.

Stutzmann GE, LaFerla FM, Parker I (2003) Ca^{2+} signaling in mouse cortical neurons studied by two-photon imaging and photoreleased inositol triphosphate. J Neurosci 23:758–765.

Taylor CW, Laude AJ (2002) IP3 receptors and their regulation by calmodulin and cytosolic Ca2+. Cell Calcium 32:321–334.

Ungless MA, Singh V, Crowder TL, Yaka R, Ron D, Bonci A (2003) Corticotropin-releasing factor requires CRF binding protein to potentiate NMDA receptors via CRF receptor 2 in dopamine neurons. Neuron 39:401–407.

Watanabe S, Hong M, Lasser-Ross N, Ross WN (2006) Modulation of calcium wave propagation in the dendrites and to the soma of rat hippocampal pyramidal neurons. J Physiol (Lond) 575:455–468.

Wilson CJ, Callaway JC (2000) Coupled oscillator model of the dopaminergic neuron of the substantia nigra. J Neurophysiol 83:3084–3100.

Wolfart J, Roeper J (2002) Selective coupling of T-type calcium channels to SK potassium channels prevents intrinsic bursting in dopaminergic midbrain neurons. J Neurosci 22:3404–3413.

Zucchi R, Ronca-Testoni S (1997) The sarcoplasmic reticulum Ca2+ channel/ryanodine receptor: modulation by endogenous effectors, drugs and disease states. Pharmacol Rev 49:1–51.